International Journal of Bio-Inorganic Hybrid Nanomaterials

Preparation of Sodium Dodecyl Sulfate Modified Pyrrolidine-1-dithiocarboxylic acid Ammonium Coated Magnetite Nanoparticles for Magnetic Solid Phase Extraction of Pb(II) from Water Samples

Sina Yekta[1*], Meysam Sadeghi[2], Esmaeil Babanezhad[3], Nooshin Shahabfar[4]

[1] *Instructor, Department of Chemistry, Faculty of Basic Sciences, Islamic Azad University, Qaemshahr Branch, Qaemshahr, Iran*

[2] *Instructor, Department of Chemistry, Faculty of Basic Sciences, Imam Hussein Comprehensive University (IHCU), Tehran, Iran*

[3] *Assistant Professor, Department of Chemistry, Faculty of Basic Sciences, Sharif University, Tehran, Iran*

[4] *Instructor, Department of Nuclear Engineering, Radiation Application, Amirkabir University, Tehran, Iran*

ABSTRACT

This paper describes the development of a procedure for Pb(II) ions removal from various water samples after magnetic solid phase extraction (MNPs) by magnetite nanoparticles (Fe_3O_4 NPs) modified with sodium dodecyl sulfate (SDS) and pyrrolidine-1-dithiocarboxylic acid ammonium (PDTCAA). The synthesis of Fe_3O_4 NPs was certified by characterization techniques including field emission scanning electron microscopy (FESEM), X-ray diffraction (XRD), Fourier transforms infrared (FTIR) spectroscopy and vibrating-sample magnetometer (VSM) and the determination process carried out by flame atomic absorption spectrometry (FAAS). Influential parameters affecting the extraction efficiency such as pH, mass of adsorbent, and amounts of modifying agents along with desorption conditions including type, concentration and least amount of the eluent were investigated and optimized. Under the optimized experimental conditions, a dynamic linear range (DLR) of 2.5-50 µg L^{-1} was obtained and the limit of detection (LOD, n = 6) and relative standard deviation (RSD %, n = 3, C = 10 µg L^{-1}) were found to be 2.5 µg L^{-1} and 2.2%, respectively. The developed method was applied for removal of Pb(II) ions from water samples.

Keyword: Magnetite nanoparticles; Pb(II) ions; Sodium dodecyl sulfate; Pyrrolidine-1-dithiocarboxylic acid ammonium; Magnetic solid phase extraction.

1. INTRODUCTION

Heavy metal distribution throughout natural water resources still remains a great issue facing the world today and it will be assumed such a great deal to remove hazardous levels of inorganics like As, Cr, Hg, Pb, Ni, Cd in diverse forms. The occurrence of these pollutants in the environment can be the cause of so many maladies especially different sorts of cancers [1, 2]. Of the most general public concerning hazards is lead which

Int. J. Bio-Inorg. Hybr. Nanomater., Vol. 3, No. 3 (2014), 143-156

Yekta S et al

has been introduced to a variety of environmental media resulting from many industrial activities such as mining, smelting, metal plating, alloy, paper and fertilizer industries, tanneries, batteries, pesticides, lead paints, coating, electroplating, petrochemical units and photographic materials production [3, 4]. The plants absorb lead from air, soil and fertilizers and it can accumulate in their tissues. Therefore lead can reach the food chain of human and other living systems [5]. Even low concentrations of lead impose serious health risks because of its bioaccumulation in live tissues throughout the food chain. Lead is commonly adsorbed to human body through inhalation, diet (contaminated food and drinking water) and skin contact [6] and it remains for a long period due to its long half-life when absorbed [7]. Lead exposure redounds various disorders, almost in each organ of body for instance brain, kidney, lungs, neurotic system [8-10]. The lower limit of lead in natural systems according to World Health Organization (WHO) is 10 μg L^{-1}. The drinking water and wastewater standard set by Environmental Protection Agency (EPA) for lead is 0.05 and 0.5 mg L^{-1}, respectively [11, 12].

The low concentrations of Pb(II) ions in industrial or environmental samples often fall below the detection limit of conventional analytical techniques such as flame atomic absorption spectrometry (FAAS) and graphite furnace atomic absorption spectrometry (GFAAS). Hence, analytical determination usually requires a preconcentration step in order to increase lead concentration. To date, different methodologies have been utilized for enriching Pb(II) ions and separate it from interferences, namely, membrane filtration [13], cloud point extraction (CPE) [14, 15], liquid–liquid extraction (LLE) [16], dispersive liquid-liquid micro-extraction (DLLME) [17, 18], liquid phase micro extraction (LPME) [19] and solid phase extraction (SPE) [20-23]. Such systems improve the sensitivity and selectivity of the determination techniques, although some of these methods found to be high cost and time consuming processes.

Over the past two decades, nanoscale materials have elicited much tendency because of their intriguing physical and chemical properties [24, 25]. These properties occur under conditions differing from those of the bulk atoms that lead to quantum effects and the increased fraction of the surface atoms as their size decreases [26, 27]. The surface atoms are unsaturated and have high chemical activity and adsorption capacity to various substances [28] while induce a minimum for internal diffusion resistance when compared to the traditional micron sized supports. Nanomaterials have particular adsorptive, electronic, optical, magnetic and catalytic properties, so they are focused in various fields of expertise [29, 30]. Nanomaterials are divided into different groups including either inorganic elements like metal and metal oxide nanoparticles (Fe_3O_4, TiO_2 and SiO_2) or organic part like carbon nanotubes- based on their role in adsorption processes which is dependent on their innate surface property and further external functionalization [31].

Magnetic solid phase extraction (MSPE) is recognized as a high yield preconcentration process which handles magnetic adsorbents like iron oxide nanoparticles, cobalt ferrite (Fe_2CoO_4) and chromium dioxide (CrO_2) [32, 33] and an outward magnetic field to separate the analytes of interest. Use of iron oxide magnetic nanoparticles (MNPs) in several types of α-Fe_2O_3, β-Fe_2O_3, γ-Fe_2O_3, ϵ-Fe_2O_3, and Fe_3O_4 as a practical adsorbent is one of the new approaches. One of the most popular magnetic materials is known as magnetite ($FeO.Fe_2O_3$) [34]. The bulk Fe_3O_4 crystallize in converse spinel structure at room temperature where the close-packed-face centered-cubic lattice is vocalized by oxygen atoms and the interstitial sites are occupied with iron atoms [35]. At room temperature magnetite transforms to maghemite [36], therefore optimization of the specific coating agents will decrease the mentioned exchanging process [37]. Magnetite nanoparticles (Fe_3O_4 NPs) are the most common type that is black in color and spherical in shape [38]. Large surface area and biocompatibility with complex matrices make Fe_3O_4 NPs unique for MSPE and overcome problems with conventional classic solid phase extraction such as packing of SPE column and long extraction time [39]. In addition to this, Fe_3O_4 NPs cannot be used in naked form. Because of their large surface to volume ratio and high surface energy; they tend to aggregate for minimizing this surface energy [40]. Naked Fe_3O_4 NPs get easily oxide in expose of air and lose magnetic properties, dispersion capability and undergo biodegradation as a result [41]. Hence,

stabilizing them via modifying agents opens the narrow window of poor behavior in extraction processes and complexation with analyts. Recent papers have proposed the use of coatings such as dithizone sodium dodecyl sulfate (DTZ/SDS) [42], 3-(trimethoxysilyl)-1-propanethiol-ethylene glycol bis-mercaptoacetate (TMSPT-EGBMA) [43], tetraethyl orthosilicate-(3-aminopropyl)trimethoxysilane (TEOS-APTMS) [44], cetyltrimethylammonium bromide (CTAB) [45], polydopamine [46] and amino group (NH_2) [47] to induce functional groups of thiol, carboxylic and amino on the surface of MNPs for the preconcentration of trace metal ions.

In present work, a Fe_3O_4 NPs-assisted MSPE procedure is optimized based on co-precipitation of ($FeCl_2.4H_2O$) and ($FeCl_3.6H_2O$) precursors and SDS-PDTCAA external functionalization for the extraction and determination of Pb(II) ions in various water samples. Also for gaining the most suitable results different factors including pH, mass of adsorbent and amounts of modifying agents along with desorption conditions such as type, concentration and least amount of the eluent were surveyed and optimized as mentioned. Moreover for optimization of these parameters, the most significant ranges were selected. To the best of our knowledge, this is the first time that SDS-PDTCAA immobilized on magmetite nanoparticles (SDS-PDTCAA-Fe_3O_4 NPs) is used for the removal of trace amounts of Pb(II).

2. EXPERIMENTAL

2.1. Chemicals

Lead (II) nitrate ($Pb(NO_3)_2$), Ferrous chloride tetrahydrate ($FeCl_2.4H_2O$), ferric chloride hexahydrate ($FeCl_3.6H_2O$), sodium dodecyl sulfate (SDS, $CH_3(CH_2)_{11}OSO_3Na$), pyrrolidin-1-dithiocarboxylic acid ammonium (PDTCAA, $C_5H_{12}N_2S_2$), acetone and sodium hydroxide were all purchased from Merck (Merck, Darmstadt, Germany). A stock solution of lead (1000 mg L^{-1}) was prepared by dissolving 1.6 g of $Pb(NO_3)_2$ in 1000 mL deionized water. Standard and working solutions of Pb(II) were prepared daily by appropriate dilution of stock solution, and all the solutions were stored in pre-cleaned polypropylene con-

tainers. Solutions of 0.002 (0.006 gr in 10 mL high purified water) mol L^{-1} SDS and 0.01 mol L^{-1} PDTCAA were prepared by dissolving the appropriate amount of these reagents in deionized water and acetone respectively. Also the stock solutions of various coexistent ions (1000 mg L^{-1}) were prepared from their nitrate or chloride salts by conventional method. All the chemicals and reagents used in present research were of analytical grade without further purification and deionized (DI) water was used for the preparation of all solutions. The pHs of the solutions were adjusted by addition of appropriate volumes of HCl or NaOH.

2.2. Apparatus

Ultrasonic experiments were performed by a Eurosonic 4D model (Euronda, Italy) for dissolving the modifying gents and synthesis of magnetic adsorbent. The synthesized Fe_3O_4 NPs were subjected to various characterization instruments. The morphology and size of Fe_3O_4 NPs were determined via SEM micrographs using field emission scanning electron microscopy (FESEM, Hitachi-S4160). The powder X-ray diffraction (XRD) patterns were recorded at room temperature using a Philips-X'Pert Pro diffractometer-MPD (Netherlands) equipped with a high power Cu-K$_\alpha$ radioactive source (λ = 1.54060 nm) at 40 kV and 30 mA to determine chemical structure and average size of the nanoparticles. Data were collected over the range 5–80° in 2θ with a scanning speed of 2° min-1. The IR spectra were scanned on a Fourier transform infrared spectrometer (FTIR, Vertex 70, Bruker) in the wavelength range of 450 to 4000 cm^{-1} using KBr pellets to identify the as prepared nanoparticles and investigate the linkage between Fe_3O_4 NPs and modifying/coating agents. Magnetic properties of the particles were determined by a LDJ9600 model vibrating sample magnetometer (VSM, Electronics Inc Troy, MI, USA). Magnetic separations were performed using a strong neodymium iron boron ($Nd_2Fe_{12}B$) magnet (10×5×4 cm, 1.4 Tesla). A M5AA system model flame atomic absorption spectrometer (Thermo, USA) equipped with an air acetylene flame and a lead hollow cathode lamp at an operating current of 15 mA was used for lead determinations. Lead ion concentration was measured using atomic absorption at wavelength of 283.3 nm and spectral bandwidth of 0.2 nm.

All measurements were based on peak height. The pH measurements were made with a Metrohm Model 774 pH meter with a combination glass electrode.

2.3. Synthesis of Fe₃O₄ NPs

In a typical preparation procedure, 9.94 g of FeCl₂. 4H₂O and 27 g of FeCl₃.6H₂O with a molar ratio of 1:2 were dissolved in 100 mL deionized water separately and added to a three-neck flask containing 160 mL deionized water, then slowly heated up to 80°C under vigorous stirring (800 rpm) using a hotplate magnetic stirrer and maintained at this temperature. 20 g of NaOH was dissolved in 100 mL deionized water and poured in a volumetric burette. Subsequently, the mixture was titrated by NaOH solution under nitrogen atmosphere until after 2 h the black precipitate magnetite was observed. Nitrogen atmosphere was used to degas the solution against oxygen to prevent the conversion of Fe₃O₄ NPs to other types of iron oxides during the synthesis procedure. During the synthesis process, the pH of the solution was maintained at about 12. The precipitates were heated at 80°C for 120 min, and then were washed several times with deionized water and ethanol. Finally, the black precipitates were dried in a vacuum oven at 60-70°C [39]. Figure 1, represents a schematic for the synthesis process.

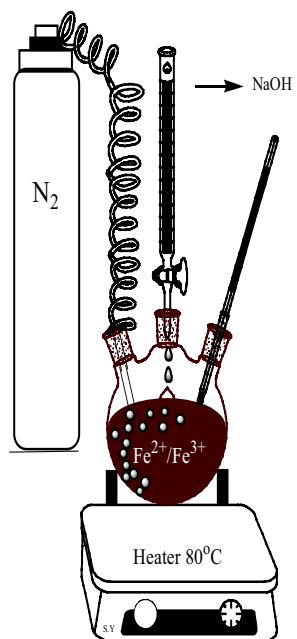**Figure 1:** *The schematic of the synthesis process of Fe₃O₄ NPs.*

2.4. Modification of Fe₃O₄ NPs

After characterization and controlling the size and morphology of the Fe₃O₄ NPs which provide particular advantages on their acts and properties in aqueous solutions including absorbance and dispersion, it sounds necessary to modify nanoparticles to gain selectivity against Pb(II) ions. MNPs should be modified due to abundant advantages improving the act of extraction process including (a) stabilize the nanoparticles in solution (b) enhancement of the nanoparticles solubility in various solvents (c) geminate the particles in specific arrays (d) Provide functional groups at the surface of MNPs (e) imprinting layers have ability to modify chemical and electronic optical properties of these particles (f) reduction of their toxicity (g) protection against oxidation [2, 12, 28 and 39]. In this work, SDS as an anionic surfactant was used as coating agent to activate their surfaces and PDTCAA was used as organic ligand to protect SDS coated-Fe₃O₄ NPs against exterior effects and provide amine functional groups on the surface of MNPs. For this purpose, 1 mL suspension (containing 0.1 g) of dried as synthesized Fe₃O₄ NPs accrued in a beaker and 0.006 g of SDS previously dissolved in 10 mL deionized water and adjusted in pH of 5 was added. The mixture was shaken and allowed to complete the coating process for 2 min in 25°C. Then the lower phase was separated by outward magnetic field provided by an Nd-Fe-B strong magnet which was placed at the bottom of the beaker. 400 µL (0.01M) of PDTCAA and 10 mL deionized water were added suddenly to the precipitated Fe₃O₄ NPs-SDS. While pH of 7 adjusted, the components were shaken for 6 min at room temperature. Again the lower solution was separated by external magnetic field in a very short time about 12 s and then dried at 60-70°C in an autoclave for 2 h until a black powder was derived. The preparation of SDS-PDTCAA-Fe₃O₄ NPs (as can be seen in Figure 2a) and adsorption of Pb(II) ions is demonstrated in Figure 2.

2.5. MSPE procedure based on Fe₃O₄ NPs

The procedure for MSPE as illustrated in Figure 2b was investigated in batch experiments and the details are as follows: Adsorption of lead from aqueous solutions was performed in an 250 mL beaker containing

10 μg L^{-1} Pb(II) ions. The pH was adjusted by drop-wise addition of 1 mol L^{-1} sodium hydroxide and 1 mol L^{-1} hydrochloric acid. 0.1 g SDS-PDTCAA-Fe$_3$O$_4$ NPs was added and the mixture was shaken for 5 min to facilitate adsorption of Pb(II) ions onto the MNPs. Using a Nd-Fe-B strong magnet, SDS-PDTCAA-Fe$_3$O$_4$ NPs were separated from the supernatant quickly where the outward magnetic field causes the aggregation of MNPs on one side of the beaker. Change in the concentration of Pb(II) ions in the solution and there upon the adsorption amounts of Pb(II) ions were measured by FAAS analysis and checked with known lead standard solutions. The magnet was removed and Fe$_3$O$_4$ NPs was settled into 1 mL of 1 mol L^{-1} HNO$_3$

as eluent to recover Pb(II) ions from the precipitate. After shaking for 5 min, magnet was used again to separate the adsorbent and the eluent was injected to FAAS to measure the concentration of desorbed lead. Extraction Percent of lead was calculated from the following equation:

$$E(\%) = \left(\frac{c_i - c_f}{c_i} \right) \times 100 \qquad (1)$$

Where C_i and C_f represent the concentration of Pb(II) ions before and after extraction in the solution, respectively. Schematic illustration of the modification of Fe$_3$O$_4$ NPs with SDS and PDTCAA groups and adsorption of Pb(II) ions.
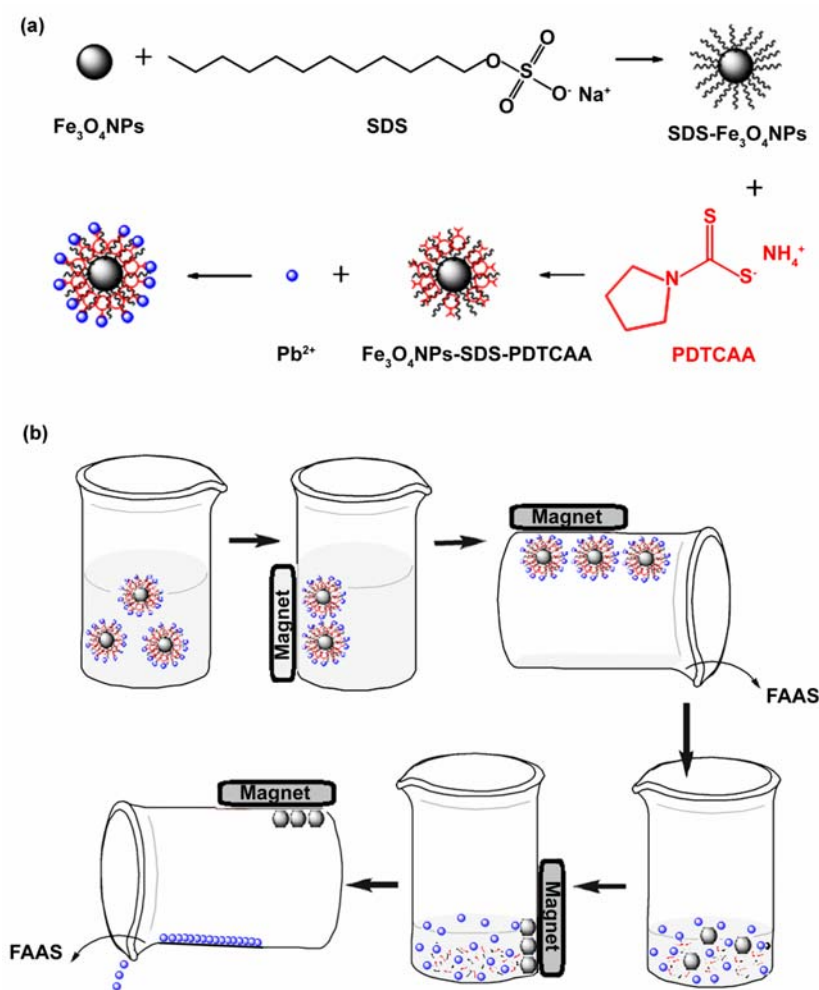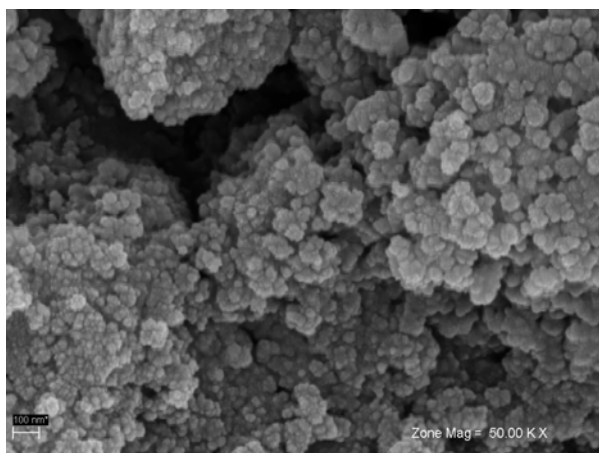

Figure 2: a) Schematic illustration of the modification of Fe$_3$O$_4$ NPs with SDS and PDTCAA groups and adsorption of Pb(II) ions, b) application of SDS-PDTCAA-Fe$_3$O$_4$ NPs for separation and preconcentration of Pb(II) ions in water samples based on MSPE.

Int. J. Bio-Inorg. Hybr. Nanomater., Vol. 3, No. 3 (2014), 143-156
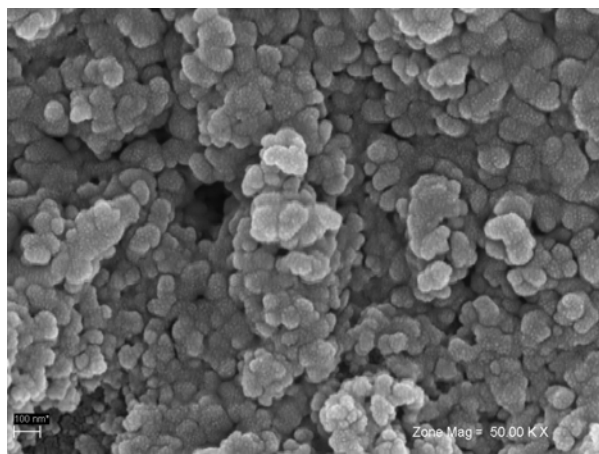
Yekta S et al

3. RESULTS AND DISCUSSION

3.1. SEM study

Size and morphology of the as synthesized MNPs were surveyed through magnification by SEM image as depicted in Figure 3a. The SEM study shows homogeneous morphology, approximately quasi-spherical shape of the nanoparticles, porous structure and also denotes that the particles morphology are retained with SDS-PDTCAA coating process which is indicated by SEM image in Figure 3b. The presence of some bigger particles in the micrographs is attributed to the aggregation or overlapping of some smaller particles during the preparation step. The average crystalline size of Fe_3O_4 NPs was demonstrated to have nanometric dimensions (less than 100 nm).
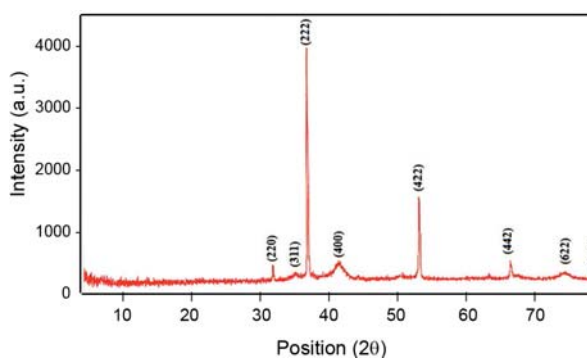

(a)

(b)

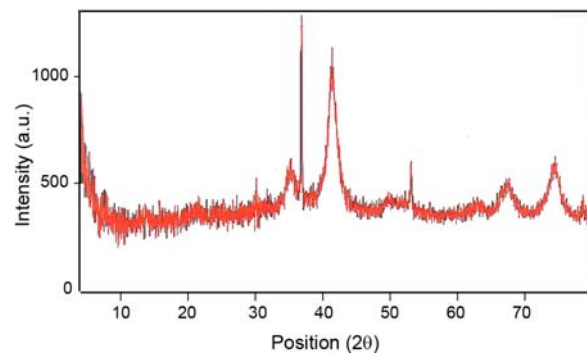**Figure 3:** SEM images of a) Fe_3O_4 NPs and b) SDS-PDT-CAA-Fe_3O_4 NPs.

3.2. XRD pattern

The crystalline structure and phase purity were determined by XRD pattern as described by Figure 4. The peaks referring to Fe_3O_4 NPs occurred at scattering angles (2θ) of 31.9001°, 35.2076°, 36.9769°, 41.4064°, 53.2888°, 66.6439°, 74.5259° and 78.7446° corresponding to diffraction planes of (220), (311), (222), (400), (422), (442), (622) and (444), respectively that have been crystallized in the cubic system with spinel structure (*Fd3m* with lattice size of 8.4000 Å, ICSD card # 01-072-2303). No characteristic peaks related to the presence of impurities were observed in the pattern during synthesis step. A definite line broadening of the scattering patterns in Figure 4 is a demonstration upon which the synthesized Fe_3O_4 NPs are in nanoscale range. The size of the prepared Fe_3O_4 NPs was investigated via XRD measurement and line broadening of the peak at 2θ = 5°-80° using Debye-Scherrer equation [48]:

$$d = \frac{0.94\lambda}{\beta \cos\theta} \qquad (2)$$

(a)

(b)

Figure 4: XRD spectrum of a) Fe_3O_4 NPs and b) SDS-PDT-CAA-Fe_3O_4 NPs.

Where d is the crystalline size, λ is the wavelength of X-ray source, β is the full width at half maximum (FWHM) and θ is Bragg diffraction angle. Using this equation, the average crystalline size in diffraction planes of (222), (422) and (442) was calculated about 64 nm. The diffraction planes of Fe_3O_4 NPs before and after coating process SDS-PDTCAA are retained which is revealed by XRD in Figure 4a and 4b. The crystalline size obtained from XRD measurement is consistent with the results from the SEM study. However, a small loss of crystallinity is observed in Figures 4b associated with the lower intensity of the peaks.

3.3. FTIR spectrum

The characterization of the prepared Fe_3O_4 NPs and the linkage with coating/modifying agents was further surveyed by FTIR spectra and the results affirm the junctions. Figure 5a depicts the FTIR spectrum of naked Fe_3O_4 NPs which have peaks around 445 cm^{-1} and 635 cm^{-1} assigned to bonding vibrations of F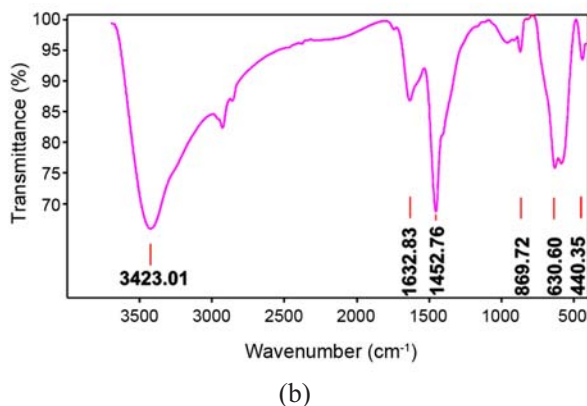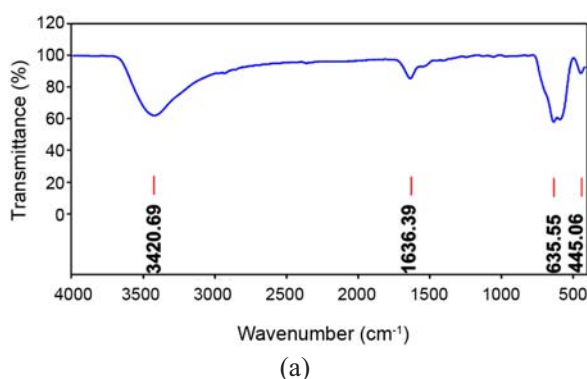e-O. The peaks appeared at 1636 cm^{-1} and 3420 cm^{-1} correspond to H–O–H bending and O–H bonding (hydroxyl groups) vibrations of nanoparticles, respectively. As plotted in Figure 4b, coated Fe_3O_4 NPs exhibits two intense peaks in 445 cm^{-1} and 630 cm^{-1} due to the stretching vibration mode associated to the metal-oxygen absorption band (Fe–O bonds in the crystalline lattice of Fe_3O_4). The bands at 869 cm^{-1} and 1452 cm^{-1} are corresponding to the S–O bending and N-H bonding vibrations belong to SDS and PDTCAA groups, respectively. The peaks around 1632 cm^{-1} and 3423 cm^{-1} are assigned to H–O–H bending and N-H bonding vibrations, respectively.

3.4. VSM

Figure 6 illustrates and compares magnetic specifications of bare Fe_3O_4 NPs and SDS-PDTCAA-Fe_3O_4 NPs via VSM magnetization curves at room temperature. VSM curves interpret and further distinguish the characteristic feature of superparamagnetism or ferromagnetism. Also regarding this technique, the maximum magnetic strength under the term saturation magnetization could be derived whose magnitude determines the power of the utilized magnet. The two curves have a similar shape and symmetry about the origin. Both bare and functionalized Fe_3O_4 NPs exhibit typical superparamagnetic behavior since no hysteresis, remanence and coercivity are observed. The saturation magnetization of bare Fe_3O_4 NPs was 76 emu g^{-1}, while as expected coating SDS-PDTCAA groups over nanoparticles lessened the quantity to 30 emu g^{-1}. This difference was due to the existence of nonmagnetic shell surrounding the magnetite nanoparticles
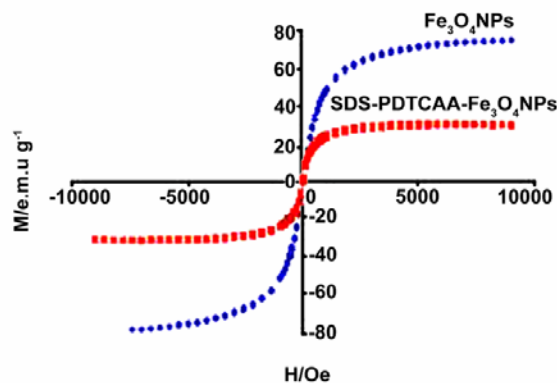

(a)

(b)

Figure 5: *FTIR spectra of a) Fe_3O_4 NPs, and b) SDS-PDT-CAA-Fe_3O_4 NPs.*

Figure 6: *The magnetic behavior of a) Fe_3O_4 NPs, and b) SDS-PDTCAA-Fe_3O_4 NPs.*

which quench the magnetic moment [49]. However, the difference was of no significance and the super-paramagnetic property of the synthesized adsorbent was sufficient for MSPE with a conventional magnet.

3.5. Analysis studies

3.5.1. Effect of pH

Of the most critical parameters influencing the extraction efficiency and adsorption capacity of SDS-PDT-CAA-Fe_3O_4 NPs is the acidity of the sample solution. In this work, the optimization of pH was assayed upon three steps: (a) SDS appending, (b) PDTCAA appending and (c) MSPE procedure. In Figure 7, the curve of ER% (extraction recovery) versus pH is shown. As depicted in this Figure, the highest adsorption characteristic of Pb(II) ions was achieved at pH ranges of 3-9 for steps a and b and 4-7 for step c. Both the metal chemistry in the solution and ionization state of modifying agents which results in the availability of adsorption sites thoroughly rely on pH. The lead retention was progressively decreased at low pHs due to the stronger interaction of H^+ ions with the adsorptive sites of SDS-PDTCAA-Fe_3O_4 NPs than that of Pb(II) ions. Protonation of SDS and PDTCAA in highly acidic conditions reduces the available ionized groups. Also at high pHs, concentration of negative charge density on the adsorbent surface results in the reduction in the SDS adsorption that together with the formation of lead hydroxide due to excess of OH- ions in basic media subsequently result in a decrease in lead adsorption. To gain the best selectivity and extraction efficiency, pHs of 5, 7 and was selected for the modification and extraction steps, respectively.

3.5.2. Effect of amount of adsorbent

Figure 8a represents the significance of the amount of adsorbent. As Fe_3O_4 NPs mass increased, extraction recoveries generally declined. This could be interpreted by the fact that with significantly high surface area and low diffusional resistance of nanoparticles, less amount of adsorbent would provide satisfactory results in extraction efficiency. On the other hand, facing with high amount of nanoparticles, the eluent would not be strong enough to recover all Pb(II) ions from adsorptive sites. Hence, 0.1 g was chosen as the appropriate mass for Fe_3O_4 NPs to fulfil high yield extraction.

3.5.3 Effect of amounts of modifying agents

Choose of appropriate amounts of both modifying agents is a key factor which affect the whole extraction and recovery process. Figure 8b, c describes the optimization for SDS and PDTCAA amounts in deionized water. Fe_3O_4 NPs accept a certain amounts of modification, so utilization of high amounts of SDS and PDTCAA might be cause of their disruption from the surface of the adsorbent into solution and ultimately formation of lead complexes within sample solution instead of Fe_3O_4 NPs surfaces. On the other hand, because of the amphiphilic properties induced via both head and tail parts of the organosulfate, SDS exhibits a micellar behavior in aqueous solutions depending on its critical micelle concentration (CMC, 8×10^{-3} mol L^{-1}). Above CMC the surface tension remains relatively constant, so SDS forms micelles and would not adsorbed on the surface of Fe_3O_4 NPs. As could be seen in Figure 8b, with increasing the amount of SDS, extraction percent of lead was increased and reached a maximum after the SDS amount approached 0.006 g in 10 mL deionized water, then a decreasing trend was observed up to CMC. Therefore, 0.006 g SDS was selected for further experiments. Also at PDTCAA volumes less than 400 μL, maximum complexation

Table 1: Effect of various inferences on Pb(II) extraction.

Coexistent ions	Permissive limit (ppm)	ER[a] (%)
Cl-	500	96.5
NO_3^-	50	97.83
SO_4^{2-}	250	100
PO_4^{3-}	50	103
NH_4^+	100	102.1
Na^+	500	95
Ca^{2+}	50	104.3
Ni^{2+}	100	105
Zn^{2+}	100	95
Cu^{2+}	50	101.3
Fe^{3+}	50	102.1
Mn^{2+}	50	95
Cd^{2+}	25	96.97
Co^{2+}	25	95
Fe^{2+}	10	95
Al^{3+}	100	95

[a] Extraction recovery

Table 2: *Analytical figures of merit of the proposed method for the extraction of Pb(II) ions.*

DLR[a]	R^2	LOD	RSD %	EF[b]	Calibration equation
(μg L^{-1})		(μg L^{-1})	(n = 3, C = 10 μg L^{-1})		
2.5-48	0.9945	2.5	2.2	250	Y = 1.403X + 0.007

[a] *Dynamic linear range;* [b] *Enrichment factor*

of Pb(II) ions cannot be achieved, since the amount of PDTCAA molecules immobilized into SDS cores is too low. For volumes more than 400 μL, overloading circumstance makes PDTCAA molecules disrupt from the surface of Fe$_3$O$_4$ NPs and lack of the adsorptive sites on the surface of Fe$_3$O$_4$ NPs decreases the extraction percent. Hence, 400 μL PDTCAA in 10 mL deionized water was chosen for further studies.

3.5.4. Effect of type, concentration and volume of the eluent
The type, concentration and least amount of the eluent was investigated to establish conditions for significantly Pb(II) ions desorption from SDS-PDTCAA-Fe$_3$O$_4$ NPs. Different eluents such as HCl, HNO$_3$, H$_2$SO$_4$ and H$_3$PO$_4$ at various concentrations and volumes were examined and the results are depicted by Figure 9. Desorption acid must not decompose the MNPs. From this point of view, concentrations and volumes higher than 3 mol L^{-1} and 3.5 mL were observed to have inverse effects on Fe$_3$O$_4$ NPs. On the other hand, the less volume for desorption will lead to higher enrichment factor. Therefore, 1 mL of 1 mol L^{-1} HNO$_3$ was found to have highest effect for quantitative recovery of adsorbed Pb(II) ions and expel them from SDS-PDTCAA-Fe$_3$O$_4$ NPs.

3.5.5. Effect of adsorption time
Lack of internal resistant, high surface to volume ratio, shorter diffusion route and the ease of separation procedure via MSPE proposed for less time even for

Table 3: *Results for the determination of Pb(II) ions in different water samples.*

Sample	Added (μg L^{-1})	Found (μg L^{-1})[a]	Relative recovery (%)
Sea water	0.0	nd[b]	102
	10.0	10.2 ± 0.2	
River water	0.0	1.3 ± 0.2	102
	10.0	11.5 ± 1.1	
Spring water	0.0	nd	96
	10.0	9.6 ± 1.8	
Well water	0.0	nd	103
	10.0	10.3 ± 2.2	
Mineral water	0.0	nd	98
	10.0	9.8 ± 1.1	
Stream water	0.0	2.2 ± 0.8	96
	10.0	9.12 ± 2.2	
waste water	0.0	3.2 ± 0.6	107
	10.0	13.9 ± 0.1	
Drinking water[c]	0.0	nd	95
	10.0	9.0 ± 0.5	
Drinking water[d]	0.0	nd	97
	10.0	9.7 ± 0.1	

[a] *Mean ± SD (n = 3);* [b] *Not detected;* [c] *Tehran city;* [d] *Ramsar city*

Table 4: *Comparison of the proposed method with some of the previously methods reported in the literature for extraction and determination of Pb(II) ions.*

Adsorbent	Method	EF	LOD ($\mu g\ L^{-1}$)	RSD (%)	References
Rice husk	FAAS	46.0	14.1	< 6	[49]
Chromosorb-102	FAAS	–	10.0	< 3	[42]
Modified ambersorb-572	FAAS	75.0	3.65	2.0	[5]
2-(2-benzothiazolylazo)-2-p-cresol-Amberlite XAD-2	FAAS	27.0	3.7	4.4-2.3	[19]
Dithizone-microcrystalline naphthalene	ICP-OES	13.3	47	2.47	[15]
naphthalene alizarin	ICP-OES	40.0	53	1.8-4.6	[6]
microcrystalline naphthalene	FAAS	200.0	2.5	2.1	[22]
Grinded eucalyptus stem	FAAS	50.0	4.5	3.6	[35]
Solid sulfur	FAAS	250.0	3.2	5.1	[38]
Methylthiosalicylate-silica gel	ICP-AES	41.0	15.3	0.9	[56]
o-Dihydroxybenzene-Silica Gel	FAAS	250.0	4.0	2.0-5.7	[51]
2-(2-thiazolylazo)-5-dimethylaminophenol-polyurethane foam	FAAS	–	2.2	6.8	[20]
poly(aminophosphonic acid)	FAAS	14.0	6.3	2.1	[53]
Multiwall carbon nanotubes	FAAS	44.2	2.6	1.4	[3]
Multiwall carbon nanotubes	FAAS	40.0	3.52	–	[17]
3-(trimethoxysilyl)-1-propanethiol-ethylene glycol bis-mercaptoacetate-Fe_3O_4 NPs	ICP-OES	236.0	0.08	4.0	[34]
SDS-PDTCAA-Fe_3O_4 NPs	FAAS	250.0	2.5	2.2	This work

larger volumes of samples. The adsorption time was surveyed in the range of 1–20 min and FAAS analysis showed that the extraction recovery first increased up to 5 min and then remained constant. Therefore, to achieve a shorter analysis time 5 min was chosen as optimum value.

3.5.6. Effect of co-existing ions

Foreign anions and cations as matrix constituents within real environmental samples may react with modifying agents and induce interference via reducing the adsorption efficiency of the target analyte. To track this effect, solutions (250 mL) containing 1 mg L^{-1} of Pb(II) ions and various amounts of coexisting ions were prepared and extracted according to the procedure described in the experimental section. Interference was considered as the deviation of ±5% from the

recovery of the standard solution. The results shown in the Table 1 point out to good selectivity of the procedure toward Pb(II) ions.

3.5.7. Analytical figures of merit

Under the optimal experimental conditions described, the linear calibration range for lead extraction obtained between 2.5 to 50 $\mu g\ L^{-1}$ (R^2 = 0.9945) for 250 mL of solution. The limit of detection (LOD) of the extraction procedure for subsequent lead analysis was found to be 2.5 $\mu g\ L^{-1}$ using LOD = 3(σ) blank/m, where σ is the standard deviation of 10 replicate measurements of blank solution and m is the slope of the calibration curve. The repeatability and precision of the method was assessed through ten adsorption/elution cycles within 250 mL sample solution containing 2.5 μg of lead. The recovery of lead as a function of sample vol-
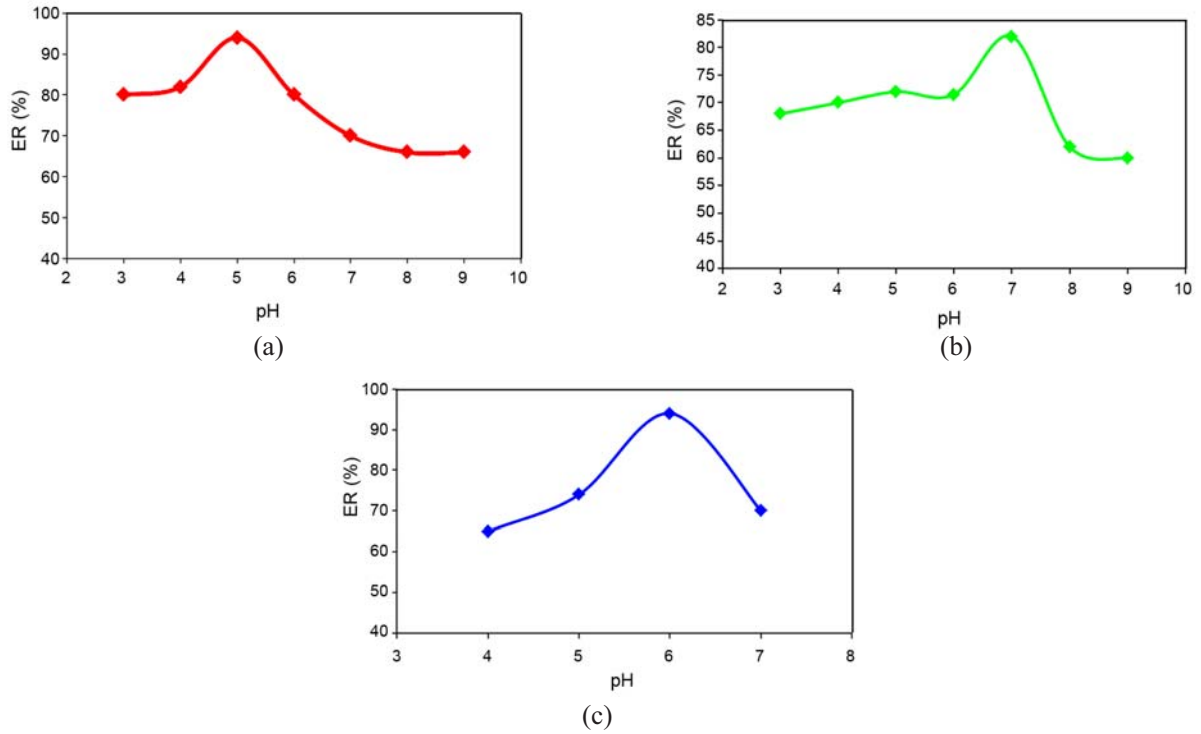
(a)

(b)

(c)

Figure 7: Effect of pH on a) SDS coating step, b) PDTCAA modification step, and c the extraction efficiency of 10 µg L^{-1} Pb(II) ions using the proposed MSPE procedure.

(a)

(b)
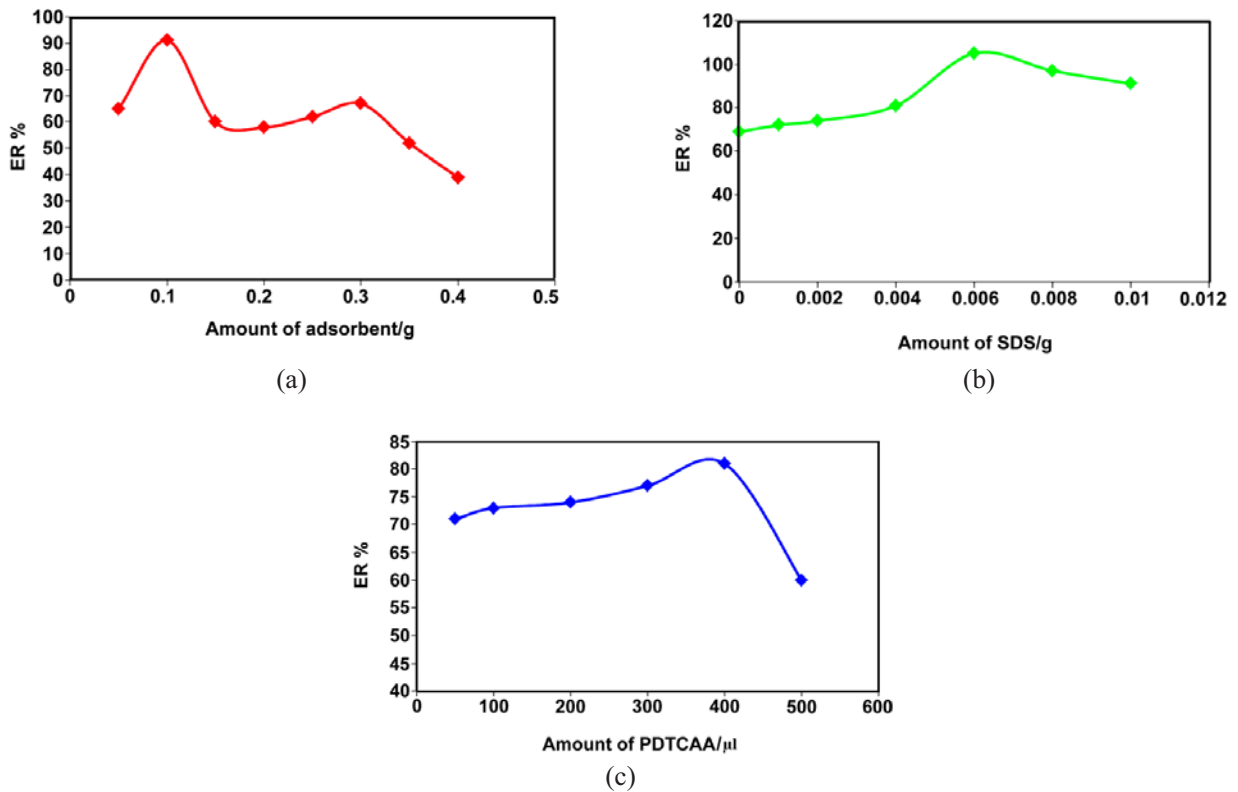
(c)

Figure 8: Effect of amount of a) SDS-PDTCAA-Fe_3O_4 NPs, b) SDS and c) PDTCAA on the adsorption characteristics of 10 µg L^{-1} Pb(II) ions using the proposed MSPE procedure.
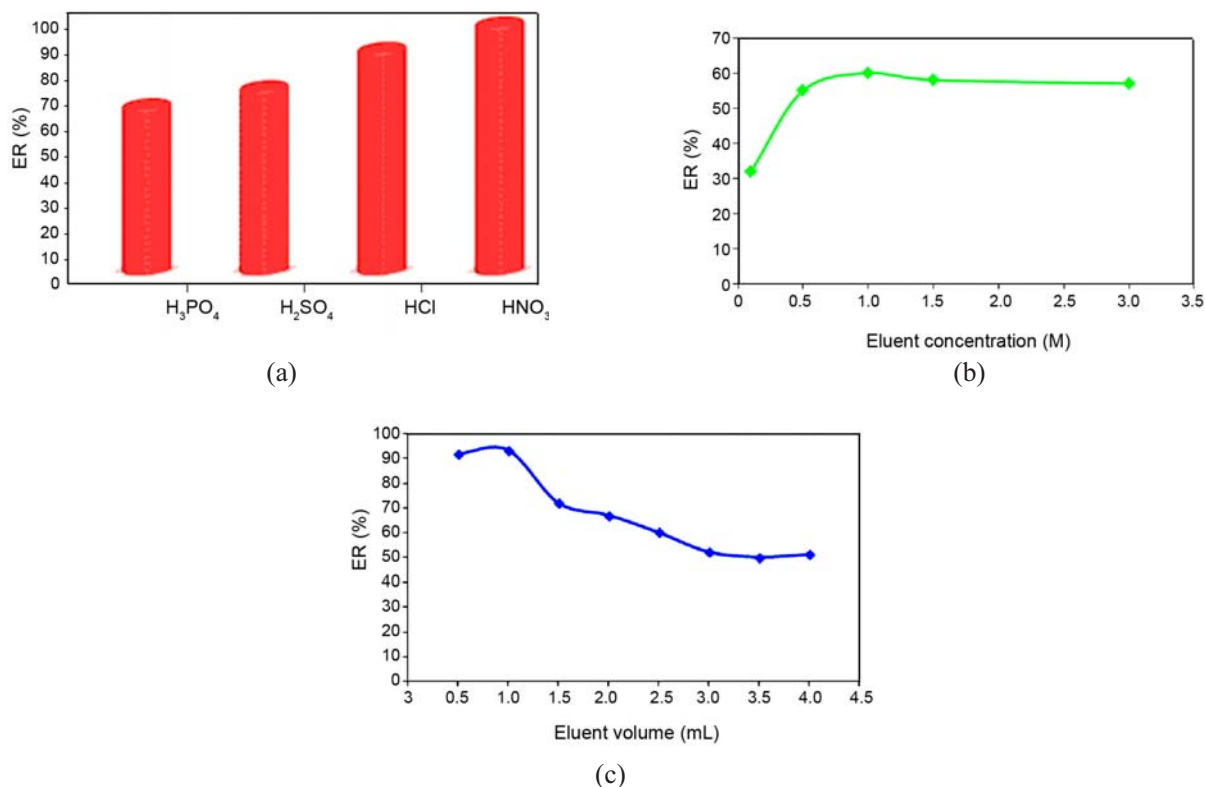
Int. J. Bio-Inorg. Hybr. Nanomater., Vol. 3, No. 3 (2014), 143-156

Yekta S et al

(a)

(b)

(c)

Figure 9: *Effect of a) type, b) concentration, and c volume of eluent (HNO_3) on the desorption characteristics of 10 µg L^{-1} Pb(II) ions from SDS-PDTCAA-Fe_3O_4 NPs using the proposed MSPE procedure.*

ume was quantitative (>95%). Whereas high recoveries were constant up to 250 mL, at higher volumes, they declined. A relative standard deviation (RSD) of 2.2% was obtained for a mean concentration of 10 µg L^{-1}. Using 250 mL sample volume and 1 mL eluent an enrichment factor of 250 was obtained. The resulting analytical characteristics are summarized in Table 2.

3.5.8. *Analytical application and validation*
The applicability and validity of the proposed MSPE procedure were assessed through real world sample analysis. Table 3 shows the mean values (n = 3) of founded amounts of Pb(II) ions and mean recoveries of 10 µg L^{-1} (2.5 µg) of spiked Pb(II) ions from 250 mL of different water samples previously adjusted pH and subjected to recommended optimizations with external calibration method. Based on three replicated analyses for each sample, results demonstrated almost quantitative percent extraction recoveries. Finally, the present method has compared with the other similar methods and the results which are denoted in Table 4

prove the capability of present method for Pb(II) extraction in different aqueous samples. ER % and Relative recovery (%) more than 100%. This can be due to high and positive relative standard deviation and sometimes the presence of interfering ions which have the wavelength very close to that of Pb(II) ions.

4. CONCLUSIONS

In this study, a MSPE method based on magnetite nanoparticles (Fe_3O_4 NPs) was successfully developed for convenient and fast lead adsorption through complexation of Pb(II) ions by SDS-PDTCAA coating/modifying groups under optimized conditions. The synthesized adsorbent was identified and characterized by employing FESEM, XRD, FTIR and VSM techniques and the extraction process followed by FAAS analysis. Magnetic separation and high surface area of nanoparticles together endue the method with high extraction capacity and enrichment factor.

The recoveries of Pb(II) ions were almost quantitative (>95%). The method is simple and proposes for sensitivity and short adsorption time for large volumes of sample solutions. The adsorbent was applied for efficient removal of Pb(II) ions from various natural and industrial water samples. The obtained results confirmed that SDS-PDTCAA-Fe_3O_4 NPs has a high potential for removal of Pb(II) ions from various aqueous samples.

ACKNOWLEDGEMENT

REFERENCES

1. Ansell R.J., Mosbach K., *Analyst*, **123** (1998), 1611.

2. Simon D.A., Diaz M., *Anal Chim Acta*, **666** (2010), 1.

3. Shao W., Chen L., Lu L., Luo F., *Desalination*, **265** (2011), 177.

4. Rahman I., Furusho Y., Begum Z.A., Izatt N., Bruening R., Sabarudin A., Hasegawa H., *Microchem J*, **98** (2011), 103.

5. Baytak S., Turker A.R., *J Hazard Mater*, **129** (2006), 130.

6. Mahmoud M.E., Yakout A.A., Abdel A.H., Osman M.M., *Bioresour Technol*, **106** (2012), 125.

7. Bouranene S., Fievet P., Szymczyk A., Hadi S.M., Vidonne A., *J Membr Sci*, **325** (2008), 150.

8. Ghaedi M., Shokrollahi A., Niknam K., Niknam E., Najibi A., Soylak M., *J Hazard Mater*, **168** (2009), 1022.

9. Citak D., Tuzen M., *Food Chem Toxicol*, **48** (2010), 1399.

10. Comitre A.L.D., Reis B.F., *Talanta*, **65** (2005), 846.

11. Liang P., Sang H., *Anal Biochem*, **380** (2008), 21.

12. Rivas R.E., Lopez G.I., Hernandez C.M., *Microchim Acta*, **166** (2009), 355.

13. Bai H, Zhou Q, Xie G, Xiao J., *Talanta*, **80** (2010), 1638.

14. Parham H., Pourreza N., Rahbar N., *J Hazard Mater*, **163** (2009), 588.

15. Li Z., Chang X, Hu Z., Huang X., Zou X., Wu Q., Nie R., *J Hazard Mater*, **166** (2009), 133.

16. Baysal A., Kahraman M., Akman S., *Curr Anal Chem.*, **5** (2009), 352.

17. Zhang L., Chang X., Li Z., He Q., *J Mol Struct*, **964** (2010), 58.

18. Liu X., Guan Y., Ma Z., Liu H., *Langmuir*, **20** (2004), 10278.

19. Qiu G., Wang Q., Wang C., Lau W., Guo Y., *Ultrason Sonochem.*, **14** (2007), 55.

20. Bhaumik M., Maity A., Srinivasu V.V., Onyango M.S., *J Hazard Mater*, **190** (2011), 381.

21. Tataru G., Popa M., Desbrieres J., *Int J pharm*, **404** (2011), 83.

22. Kalfa O.M., Yalcinkaya O., Turker A.R., *J Hazard Mater*, **166** (2009), 455.

23. Singh S., Barick K.C., Bahadur D., *J Hazard Mater*, **192** (2011), 1539.

24. Hennion M.C., *J Chromatogr A*, **856** (1999), 3.

25. Khajeh M., Laurent S., Dastafkan K., *Chem Rev*, **113** (2013), 7728.

26. Cabuil V., 2002. *Encyclopedia of Surface and Colloid Science*, Marcel-Dekker Inc., New York.

26. Cabuil V., *Marcel Dekker Inc, New York*, (2002), 4306.

27. Yang J., Lee H., Hyung W., Park SB., Haam S., *J Microencapsul*, **23** (2006), 203.

28. R.M. Cornell, U. Schwertmann, 1996. *The iron oxides*, Wiley, New York.

29. Jeng H.T., Guo G.Y., *Phys Rev B*, **65** (2002), 094429.

30. Tartaj P., del Puerto M.M., Veintemillas-Verdaguer S., Gonzalez-Carreno T., Serna C., *J. Phys D Appl Phys*, **36** (2003), 182.

31. R.M. Cornell, U. Schwertmann, 2003. *The iron oxides: structure, properties, reactions, occurrences, and uses*, 2nd edn. Wiley-VCH, Weinheim.

32. Muller R., Dutz S., Habisreuther T., Zeisberger M., *J Magn Mater*, **323** (2011), 1223.

33. Kassaee M.Z., Motamedi E., Majidi M.M., *Chem Eng J*, **172** (2011), 540.

34. Mansour S.F., *J Magn Mater*, **323** (2011), 1735.

35. Cabuil V., Dupuis V., Talbot D., Neveu S., *J Magn*

Int. J. Bio-Inorg. Hybr. Nanomater., Vol. 3, No. 3 (2014), 143-156

Yekta S et al

Mater, **323** (2011), 1238.

36. Karimi M.A., Hatefi-Mehrjardi A., Mohammadi S.Z., Mohadesi A., Mazloum-Ardakani M., Hormozi Nezhad M.R., Askarpour Kabir A., *J Iran Chem Soc*, **9** (2012), 171.

37. Mashhadizadeh M.H., Amoli-Diva M., Shapouri M.R., Afruzi H., *Food Chem.*, **151** (2014), 300.

38. Zhang J., Zhai S., Li S., Xiao Z., Song Y., Qingda A., *Tian G. Chem Eng J*, **215** (2013), 461.

39. Faraji M., Shariati S., Yamini Y., Adeli M., *Arab J Chem.*, (2012), http://dx.doi.org/10.1016/j.arabjc.2012.10.012.

40. Buendia S., Cabanas G., Alvarez–Lucio G., Montiel-Sanchez H., Navarro-Clemente M.E., Corea M., *J Colloid Interface. Sci.*, **354** (2011), 139.

41. Tan Y., Chen M., Hao Y., *Chem Eng J*, **191** (2012), 104.

42. Patterson A., *Phys. Rev*, **56** (1939), 978.

43. Ngomsik A.F., Bee A., Siaugue J.M., Talbot D., Cabuil V., Cote G., *J Hazard Mater*, **166** (2009), 1043.

44. Tarley C.R.T., Ferreira S.L.C., Arruda M.A.Z., *Microchem J*, **77** (2004), 163.

45. Saracoglu S., Elçi L., *Anal Chim Acta*, **452** (2002), 77.

46. Ferreira S.L.C., lemos V.A., Santelli R.E., Ganzarolli E., Curtius A.J., *Microchem J*, **68** (2001), 41.

47. Costa A.C.S., Lopesa L., Korn M.G.A., Portela J.G., *J Braz Chem Soc*, **13** (2002), 674.

48. Bispo M.S., Korn M.G.A., Morte E.S.B., *Spectrochim Acta B*, **57** (2002), 2175.

49. Qu J, Liu G, Wang Y, Hong R, *Adv. Powder. Technol*, **21**, (2010), 461.

50. Gopi K.P., Rao K.S., Biju V.M., Prasada R.T., Naidu G.R.K., *Chem Anal*, **49** (2004), 383.

51. Mousavi H.Z., Aibaghi E.B., Arjmandi A., *J Chin Chem Soc*, **56** (2009), 974.

52. Zougagh M., García de T.A., Vereda A.E., Cano J.M., *Talanta*, **62** (2004), 503.

53. Venkatesh G, Singh A.K., Venkataramani B., *Microchim Acta*, **144** (2004), 233.

54. Ferreira S.L.C., Santos W.N.L., Bezerra M.A., Lemos V.A., Bosque-Sendra J.M., *Anal Bioanal Chem*, **375** (2003), 443.

55. Yebra-Biurrun M.C., Enriquez-Domínguez M.F., García-Garrido A., Moreno-Cid A., *Talanta*, **21** (2000), 225.

56. Barbosa A.F., Segatelli M.G., Pereira A.C., Santos A.S., Kubota L.T., Luccas P.O., Tarley C.R., *Talanta*, **71** (2007), 1512.

57. Duran A., Tuzen M., Soylak M., *J Hazard Mater*,